Application of ground shaking scenarios to PSHA and risk assessment in near field

M. Villani
Rose School, IUSS PAVIA, Via Ferrata, 1 – Pavia (Italy) mvillani@roseschool.it

K. Demartinos, M. Vanini, E. Faccioli
Department of Structural Engineering – Politecnico di Milano, Piazza L. da Vinci, 32 -20133 Milano

ABSTRACT:
The study illustrates probabilistic ground shaking hazard analyses and risk assessment in the near field of a rupturing earthquake fault, where the datasets underlying most ground motion predictive equations (GMPEs) tend to provide insufficient coverage. In order to overcome this limitation, explicit modeling of source and wave propagation at the sites of interest can be used. 3D deterministic simulations (limited to frequencies < 2 Hz) are performed, using the spectral element code GEOELSE, and integrated with an appropriate high frequency contribution generated with a stochastic finite-fault model (EXSIM code). We show how the resulting broad-band time histories of ground motion can be introduced in PSHA, as an alternative input to the GMPEs, and we compare the derived seismic hazard curves with the results of the traditional approach. The capabilities of the CRISIS2008 code are exploited for this purpose. In seismic risk analysis, the simulated time histories and associated response spectra are treated as realizations of a random variable that represents ground motion and depends on the uncertain fault parameters, in order to evaluate probable damage of classes of buildings through Monte-Carlo approximation. An application to the seismically active area of Sulmona town, in Central Italy, is illustrated.

Keywords: numerical simulations, generalized attenuation descriptors, PSHA, damage assessment

1. INTRODUCTION

The object of probabilistic seismic hazard analysis (PSHA) is the evaluation of annual frequencies of exceedance of ground motion levels at a site. The result is a seismic hazard curve (annual probability of exceedance vs. ground motion amplitude) or a uniform hazard spectrum (spectral amplitude vs. structural period, for a fixed annual probability of exceedance). A key ingredient of any PSHA is the description of the ground motion attenuation. To this end, generally, empirical ground-motion models are used, that describe the distribution of expected ground motion parameters as a function of a few independent parameters, such as magnitude, source-to-site distance and site classification. However, reference datasets of most ground motion predictive equations (GMPEs) tend to be insufficient in the near field of the source, so that uncertainties in estimations are typically quite large and hence the use of numerical simulation appears an appealing alternative. A sufficient number of source and wave propagation simulations for random realizations of source parameters would allow for the calculation of the first two (or three) statistical moments for the ground motion parameter of interest. These moments can be subsequently introduce into PSHA. However, the concept of an integrated probabilistic- deterministic approach to seismic hazard assessment (SHA) is not new. It was proposed by Convertito et al. (2006), who used a predominantly far field approximation for generating the deterministic ground motions. Moreover within the SCEC's CyberShake Project (Graves *et al*., 2010) 3D simulations and finite fault rupture descriptions in the low frequency range have been used to compute seismic hazard analyses in Southern California. Within the Italian Project S2 "Development of a dynamical model for seismic hazard assessment at national scale" (http://nuovoprogettoesse2.stru.polimi.it), instead, emphasis is placed on generating broadband deterministic ground shaking near the earthquake source, where directivity effects might render the existing building stock more vulnerable.

Herein, we describe the method developed to this respect and we illustrate a first application on the Sulmona basin in Central Italy. Finally, the simulated ground motion is used to evaluate probable damage of classes of buildings through Monte-Carlo approximation.

2. GROUND MOTION NUMERICAL SIMULATIONS OF SULMONA BASIN

2.1. 3D numerical simulations

This basin, located in a mountain region of Central Italy, is bordered to the E by the Mt. Morrone Fault, which is about 20 km long with a depth between 1 and 11.6 km and characterized by normal kinematics. The estimated slip rate is of about 0.5-0.6 mm/yr (Barchi et al. 2000) while the maximum magnitude attributed by the Italian database of active faults DISS3 (DISS Working Group, 2009) is Mw 6.4.

The 3D simulations of seismic wave propagation within the Sulmona basin were carried out with the code GeoELSE (http://geoelse.stru.polimi.it), based on the spectral element approach developed by Faccioli et al. (1997), implemented in parallel computer architectures, and duly tested in the international benchmark for earthquake ground motion numerical simulations in the Grenoble Valley, France (Stupazzini et al., 2009). The spectral mesh, displayed in Figure 1, consists of 370,857 elements ranging in size from about 100 m, inside the basin, to 900 m in the deepest rock formation. The element size is designed to propagate frequencies up to around 3 Hz, with spectral degree 3.

30 numerical simulations were carried out by randomly selecting the hypocenter location inside the fault plane, and by coupling it with a slip distribution chosen among 21 pre-selected patterns. Should the source parameters be represented by a vector **Z**, every simulation could be interpreted as a random realization thereof. An example of the slip distribution is also shown in the right side of Figure 1. For details on the specific model, see Faccioli et al. (2010a).

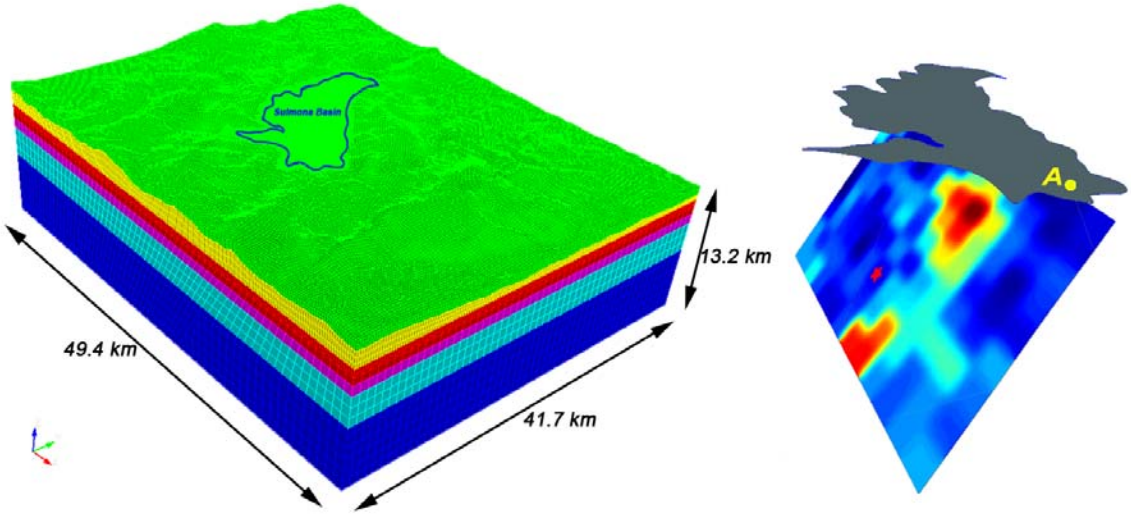

Figure 1. Left panel: 3D hexahedral spectral element mesh adopted for the simulations of the Sulmona case study. Right panel: 2D view of the alluvial basin and of the fault and example of one of the slip distributions selected for the case study. The location of the investigated receiver (A) is also shown.

2.2. Integration with high frequency content

The limited resolution of the 3D numerical algorithm implies that the resulting accelerograms do not contain harmonic components for frequencies larger than 2 *Hz*. For damage evaluation purposes, however, these need to be integrated into higher frequencies. This has been achieved, through finite-fault stochastic simulations (EXSIM, Motazedian and Atkinson 2005), generating broadband signals *A(f)* according to the following scheme:

$$A(f) = w_{LF}(f)A_{LF}(f) + w_{HF}(f)A_{HF}(f), \tag{2.1}$$

where $A_{LF}(f)$ and $A_{HF}(f)$ denote the Fourier transform of the ground acceleration produced through the 3D simulations and EXSIM respectively, whereas $w_{(.)}$ represent ad-hoc weighting functions.
The stochastic simulations introduce an additional level of uncertainty, since, for a given combination of slip distribution and hypocenter location, each synthetic motion produced by EXSIM is essentially based on a single realization of a suite of white-noise vectors **W** corresponding to the constituent sub-faults of the fault examined. This problem has been managed with the consideration of multiple realizations of **W**, which may serve as an artificial sample for further statistical analysis in a probabilistic context.

3. PSHA ANALYSIS

S2 project aimed at designing, testing and applying an open-source code for seismic hazard assessment (SHA), that could be able to inject in the hazard computations the knowledge related both to the time-dependent earthquake occurrence models and to the description of attenuation. These objectives have been pursued through the extension of the existing, widely used SH code CRISIS2007 (Ordaz et al., 1991). The new code (CRISIS2008) allows, among the other options, to handle the results of the numerical simulations toward a generalized description of attenuation. While ground motions descriptions obtained through traditional attenuation models (GMPE) are generally functions of earthquake magnitude and source-to-site distance, the generalized attenuation functions (GAF) are simply probabilistic "footprints" of the ground motions produced by an individual event. Hence, in order to use the results of the ground motion simulations as inputs of the PSHA, the moments and the probability density function underlying the simulated data should be identified. Once the distribution function is chosen, the first two statistical moments from the population of ground motion simulations (at the sites of interest) can be computed and used in the same way as one would use the median and the standard error provided by a GMPE.

3.1 Choice of a probability distribution for the numerical spectral ordinates

The continuous probability distributions to be considered are, in principle, those presently included in the software (CRISIS2008), i.e. the normal, the lognormal, the gamma and the beta distributions. However, the normal and the beta are excluded because they cannot appropriately fit the observed data, and the tests were focused on the lognormal and the gamma distributions. Three different tests have been performed: (1) visual tests, that graphically compare the observed data with the density and the cumulative functions of the selected probability distributions; (2) goodness-of-fit tests, and in particular the Kolmogorov-Smirnov (K-S) test, the Chi-square (X^2) test and the Anderson-Darling (A-D) test and finally (3) comparison of the statistical moments computed from the samples and the theoretical moments from the selected distributions. The tests, performed at different locations and for different site conditions, show that both the lognormal and the gamma distributions well fit the simulated data. Therefore, in the following the lognormal distribution is assumed as the probability density function underlying the representative shaking parameters computed through the simulations.

3.2 Results

In direct analogy with the numerical simulations, the PSHA is carried out considering only the Sulmona fault. The seismic activity of the fault source was treated with the Brownian Passage Time (BPT) occurrence model in which the mean recurrence intervals are evaluated indirectly, by treating separately the uncertainties in slip rate assignment, and in the characteristic magnitude (Peruzza et al., 2008). The probability of occurrence of the characteristic earthquake (M_w=6.4) on the Mt. Morrone fault is of 0.063 in the next 30 years. The CRISIS2008 option for which "source ruptures entirely" has been selected. With the same fault geometry and target magnitude, PSHA was also executed with two traditional GMPE computed for soil type B: Faccioli et al. (2010), denoted as FEA10, and Boore and Atkinson (2008), or BA08.
Figure 2 illustrates the hazard results in terms of uniform hazard (UH) spectra in Sulmona (receiver "A" in Figure 1). The UH displacement (left panel) and acceleration (right panel) spectra with a probability of exceedance of 3% in 30 years (roughly corresponding to 975 years of return period) derived by adopting the GAF are compared with the ones obtained by using the BA08 model and the

FEA10 model. The use of GAF leads to larger spectral values due to the combination of fault rupture and basin amplification effects (in particular at longer vibration periods) that are not typically included in classical attenuation relations. Finally it can be highlighted that at short period (UH acceleration spectra) the FEA10 model predicts almost the same levels of hazard than the GAF, while BA08 gives lower values.

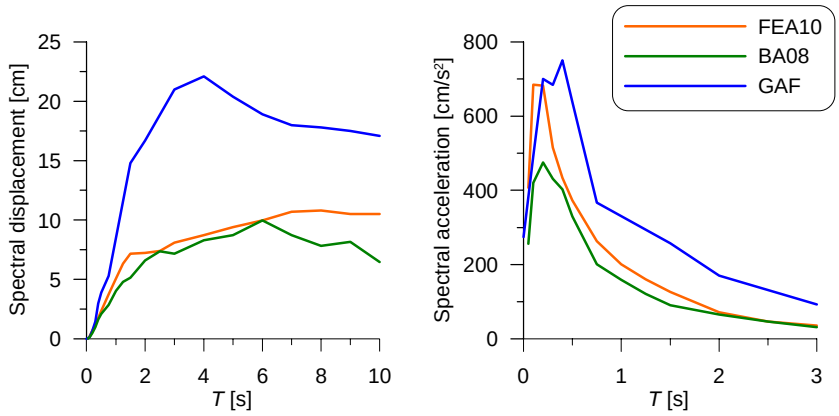

Figure 2. Comparison of the uniform hazard (UH) displacement (left panel) and acceleration (right panel) response spectra obtained with CRISIS2008 by using generalized attenuation functions (GAF), blue curve, the attenuation model of Faccioli et al. 2010, (FEA 10, orange curve) and the one of Boore and Atkinson 2008 (BA08, green curve) for the probability of exceedance of 3% in the next 30 yr.

4. PROBABILISTIC EVALUATION OF DAMAGE RISK OF CLASSES OF BUILDINGS

4.1. Methodology

To quantify damage risk for classes of buildings the capacity-demand diagram method (Chopra and Goel, 1999) is used. In this context, seismic performance is quantified through the displacement D_{pp} at the intersection of capacity diagram and the demand diagram, depicted in Figure 3(a). For the evaluation of the capacity diagram, which typically assumes a bilinear form, it suffices to derive the initial period T_0, the yield acceleration A_y (and subsequently the yield displacement D_y) and the ultimate displacement capacity, D_u of the structural system considered. This is feasible though conventional pushover analysis or using simplified mechanical models (see Calvi et al. 2006 for an overview).

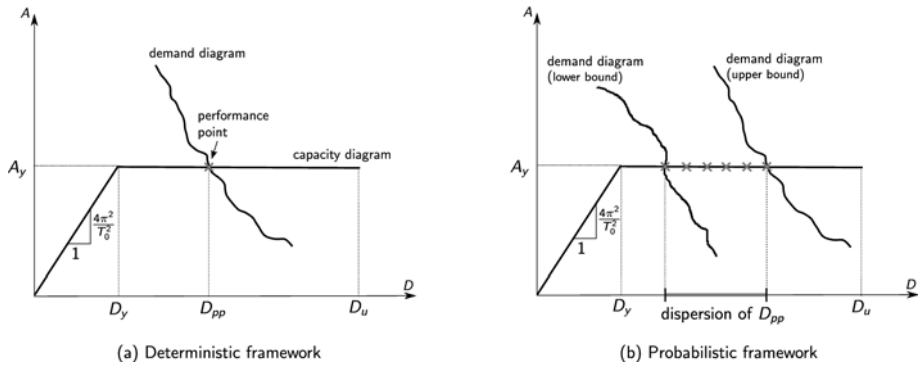

Figure 3. Capacity demand-diagram method

The demand diagram is a plot of spectral displacement and spectral pseudo-acceleration and thus relates to the structural system and the ground motion. When multiple ground-motion realizations are possible for an earthquake scenario, the performance of the structure manifests some variability due to the dispersion of D_{pp}, as can be seen in Figure 3(b).

Seismic demand is formally expressed as the response of an inelastic system of initial period T_0

following a selected hysteresis rule, for successive levels of inelastic deformation, in terms of maximum ductility. This implies the generation of a constant-period demand diagram (CPDD). For a given time-history acceleration, the value of D_{pp} can be thus interpreted as the inelastic spectral displacement of a system of initial period T_0 assuming a strength reduction factor R_{ypp} given by

$$R_{y_{pp}}\left(T_{0,}A_y\right)=\frac{S_{ae}\left(T_0\right)}{A_y} \tag{4.1}$$

where S_{ae} denotes the elastic spectral pseudo-acceleration, considering that A_y represents acceleration demand as well as acceleration capacity. Let S_{di} denote inelastic spectral displacement, then D_{pp} can be expressed as follows:

$$D_{pp} = S_{di}\left(T_0, R_{y_{pp}}\right). \tag{4.2}$$

4.2. Probabilistic Formulation

Seismic risk is quantified through the probability $P_{f,k}$ that the displacement at the performance point D_{pp} is larger than prescribed thresholds D_k of structural inelastic deformation that signify the occurrence of discrete damage limit states k, for k = 1, 2, 3, 4. That is,

$$P_{f,k} = P\left(D_k < D_{pp}\right) \tag{4.3}$$

A definition of the limit states has been suggested by Calvi (1999), in terms of the level of structural and non-structural damage, whereas nominal values for D_k have been proposed in Pagnini et al. (2008).

To treat the range of uncertainties related to the ground motion, S_{ae} is expressed as a function of the vector **Z** that represents the fault parameters in the 3D simulations and the set of vectors **W** that comprise the stochastic part of the EXSIM method. These random vectors are by definition independent. Hence, using the total probability theorem and considering Eqn. (4.1) and Eqn. (4.3), $P_{f,k}$ can be expanded as follows:

$$P_{f,k} = \iint_{\mathbf{z}\,w} P\left(D_k < D_{pp}\left(\mathbf{Z}=\mathbf{z},\mathbf{W}=\mathbf{w}\right)\right) f_{\mathbf{W}}\left(\mathbf{w}\right) f_{\mathbf{Z}}\left(\mathbf{z}\right) d\mathbf{w}\, d\mathbf{z}\,, \tag{4.4}$$

where lowercase letters denote realizations of the respective random variables, while the associated probability density functions are represented by $f_{(\cdot)}$. Let n_z and n_w denote the number of realizations of the vectors **Z** and **W** respectively, then the integral in Eqn. (4.4) can be calculated through Monte-Carlo approximation as follows:

$$P_{f,k} \approx \frac{1}{n_z}\sum_{i=1}^{n_z}\frac{1}{n_w}\sum_{j=1}^{n_w} P\left(D_k < D_{pp}\left(\mathbf{z}_i, \mathbf{w}_j\right)\right). \tag{4.5}$$

The knowledge of $P_{f,k}$ leads to the evaluation of the probability of occurrence of the k^{th} limit state, $P_{d,k}$. If the value k = 0 is used to represent a dummy limit state, in which any structural and non-structural damage is absent, then

$$\begin{aligned} P_{d,0} &= 1 - P_{f,1} \\ P_{d,k} &= P_{f,k-1} - P_{f,k} \quad \text{for } k = 1,2,3. \\ P_{d,4} &= P_{f,4} \end{aligned} \tag{4.6}$$

The probability measure $P_{d,k}$ may be interpreted as the probability that the damage level associated to the *k-th* limit state is observed.

4.3. Example of Application

The method has been implemented on the population of 4-Storey masonry buildings constructed before 1919 in the town of Sulmona, Italy, using the simplified mechanical model proposed by Pagnini et al. (2008). It is evident that the consideration of uncertainty in the ground motion leads to the dispersion of the performance points, as illustrated in Figure 4(a). There are many realizations that produce values of D_{pp} significantly larger than the ultimate displacement of the structural system considered. This results in large probability measures for the occurrence most adverse levels of damage, i.e. $k > 3$, as can be observed in Figure 4(b).

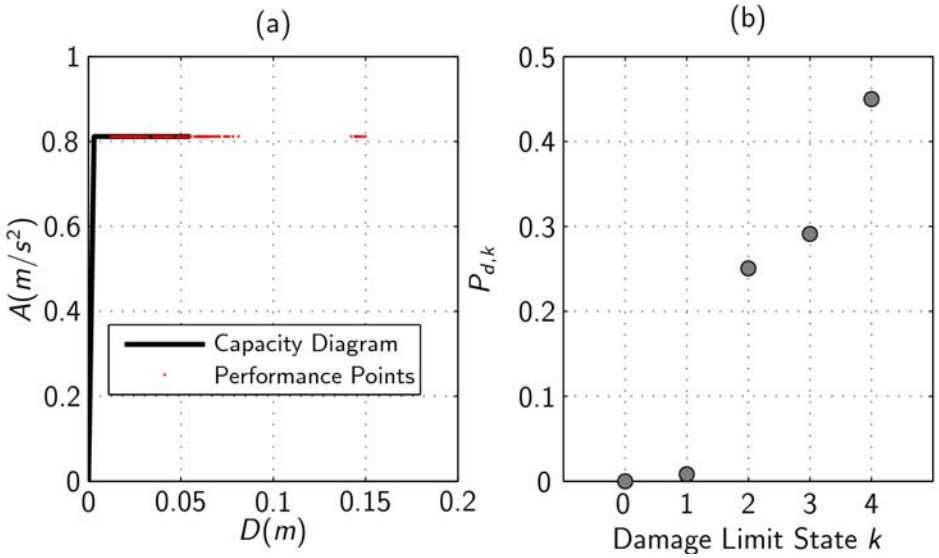

Figure 4. (a) Capacity diagram and performance points. (b) Probability of Damage

5. CONCLUSIONS

In this paper, we have discussed the use of synthetic near field ground motion produced through 3D simulations of wave propagation into PSHA and damage risk assessment.

In order to overcome the limitations of the classical GMPEs, generalized descriptions of attenuation may be used for local studies, for which the hazardous earthquakes are few and can be clearly identified. In this case, the geographical distribution of statistical moments of one or more intensity measures for each event can be defined using, for instance, advanced ground-motion simulation techniques. Uniform hazard spectra obtained with this approach are compared with those resulting by using two classical GMPEs, showing, generally, larger spectral values. This behaviour can be justified by the observation that site effects, basin effects and also topographic effects are more realistically accounted for with the numerical simulations.

Synthetic ground motion representing random rupture realizations of an earthquake scenario can be directly treated in a probabilistic context through the use of Monte Carlo simulations. This allows to quantify the effects of ground motion variability on structural damage of classes of buildings as illustrated in the study case of Sulmona town (Italy).

AKCNOWLEDGEMENT

This work was supported by the S2 project “Development of a dynamical model for seismic hazard assessment at national scale” of the 2007-2009 agreement between the Department of Civil Defence of Italy and INGV.

REFERENCES

Barchi, M., Galadini, F., Lavecchia, G., Messina, P., Michetti, A., Peruzza, L., Pizzi, A., Tondi, E. and Vittori, E. (2000). Sintesi delle conoscenze sulle faglie attive in Italia Centrale: parametrizzazione ai fini della caratterizzazione della pericolosità sismica, Volume congiunto dei Progetti 5.1.2, 6a2, 5.1.1, CNR-GNDT, Rome.

Boore, D.M., and Atkinson, G.M., (2008). Ground-motion prediction equations for the average horizontal component of PGA, PGV, and 5%-damped PSA at spectral periods between 0.01 s and 10.0 s, Earthquake Spectra, 24(1), 99-138.Calvi, G. (1999). A Displacement-based Approach for Vulnerability Evaluation of Classes of Buildings. Journal of Earthquake Engineering. 3:3, 411–438.

Calvi, G., Pinho, R., Magenes, G., Bommer, J., Restrepo-Vélez, L., and Crowley, H. (2006). Development of Seismic Vulnerability Assessment Methodologies over the past 30 Years. ISET Journal of Earthquake Technology. 43:3, 75–104.

Chopra, A. K. and Goel, R. K. (1999). Capacity-Demand-Diagram Methods Based on Inelastic Design Spectrum. Earthquake Spectra. 15:4, 637–656.

Convertito, V., Emolo, A., and Zollo A., (2006), Seismic-Hazard Assessment for a Characteristic Earthquake Scenario: An Integrated Probabilistic–Deterministic Method, *Bull. Seism. Soc. Am.* **96**:2 , 377-391.

DISS Working Group, 2009. Database of Individual Seismogenic Sources (DISS), Version 3.1.0: A compilation of potential sources for earthquakes larger than M 5.5 in Italy and surrounding areas. http://www.ingv.it/DISS/, © INGV 2009 - Istituto Nazionale di Geofisica e Vulcanologia - All rights reserved.

Faccioli, E., Vanini, M., Villani, M., Cauzzi, C. and Smerzini, C. (2010a). Mapping seismic hazard to account for basin amplification effects, *9th International Workshop on Seismic Microzoning Risk Reduction*, C*uernavaca, México.*

Faccioli, E., Bianchini, A., Villani, M., (2010). New ground motion prediction equations for T > 1 s and their influence on seismic hazard assessment. *The university of Tokyo Symposium on long period ground motion and urban Disaster mitigation, University of Tokyo, Japan,March 17-18, 2010.*

Faccioli, E., F. Maggio, R. Paolucci and A. Quarteroni (1997). 2D and 3D elastic wave propagation by a pseudo-spectral domain decomposition method, *Journal of Seismology*, **1**, *237-251.*

Graves, R., Callaghan, S., Small, P., Mehta, G., Milner, K., Juve, G., Vahi, K., Field, E., Deelman, E., Okaya, D., Maechling, P., Jordan, T.H. (2010), Full waveform physics-based probabilistic seismic hazard calculations for Southern California using using the SCEC CyberShake platform. *The university of Tokyo Symposium on long period ground motion and urban Disaster mitigation, University of Tokyo, Japan,March 17-18, 2010.*

Motazedian, D. and Atkinson, G. M. (2005). Stochastic Finite-Fault Modeling Based on a Dynamic Corner Frequency. Bulletin of the Seismological Society of America. 95:3, 995–1010.

Ordaz, M., Jara, J.M., Singh, S.K. (1991) Riesgo sísmico y espectros de diseño en el estado de Guerrero. Technical Report, Instituto de Ingenieria, UNAM, Mexico City.

Pagnini, L., Vicente, R., Lagomarsino, S., and Varum, H. (2008) A Mechanical Method for the Vulnerability Assessment of Masonry Buildings. 14th World Conference on Earthquake Engineering. DVD Proceedings.

Peruzza, L., Pace, B., Cavallini, F. [2008] "Error propagation in time-dependent probability of occurrence for characteristic earthquakes in Italy", Journal of Seismology, DOI 10.1007/s10950-008-9131-1.

Stupazzini, M., Paolucci, R. and Igel, H. (2009). Near-fault earthquake ground motion simulation in the Grenoble Valley by a high-performance spectral element code. *Bull. Seism. Soc. Am.* **99**: ,286-301.